AGU ADVANCING EARTH AND SPACE SCIENCES

Geophysical Research Letters

RESEARCH LETTER
10.1029/2023GL107508

Structure of the Bottom Boundary Current South of Iceland and Spreading of Deep Waters by Submesoscale Processes

Charly de Marez[1], **Angel Ruiz-Angulo**[1], **and Mathieu Le Corre**[2,3]

[1]University of Iceland, Reykjavik, Iceland, [2]Service Hydrographique et Océanographique de la Marine (SHOM), Brest, France, [3]Laboratoire d'Océanographie Physique et Spatiale (LOPS), University of Brest, CNRS, IRD, Ifremer, IUEM, Brest, France

Key Points:

- An intense bottom boundary current originating from the Iceland-Faroe Ridge and the Faroe Bank Channel flows along the Icelandic Shelf
- The rough topography and the intensity of the current lead to bottom mixing and sustain a large bottom mixed layer
- Subsmesoscale structures generated locally participate in the spreading of deep water masses in the Iceland Basin

Supporting Information:

Supporting Information may be found in the online version of this article.

Correspondence to:

C. de Marez,
charly@hi.is

Citation:

de Marez, C., Ruiz-Angulo, A., & Le Corre, M. (2024). Structure of the bottom boundary current south of Iceland and spreading of deep waters by submesoscale processes. *Geophysical Research Letters*, *51*, e2023GL107508. https://doi.org/10.1029/2023GL107508

Received 29 NOV 2023
Accepted 15 FEB 2024

Author Contributions:

Conceptualization: Charly de Marez, Angel Ruiz-Angulo
Formal analysis: Charly de Marez
Funding acquisition: Angel Ruiz-Angulo
Methodology: Charly de Marez
Project administration: Angel Ruiz-Angulo
Software: Charly de Marez, Mathieu Le Corre
Supervision: Angel Ruiz-Angulo
Validation: Angel Ruiz-Angulo, Mathieu Le Corre
Visualization: Charly de Marez
Writing – original draft: Charly de Marez

Abstract The northeastern part of the North Atlantic subpolar gyre is a key passage for the Atlantic Meridional Overturning Circulation upper cell. To this day, the precise pathway and intensity of bottom currents in this area is not clear. In this study, we make use of regional high resolution numerical modeling to suggest that the main bottom current flowing south of Iceland originates from both the Faroe-Banks Channel and the Iceland-Faroe Ridge and then flows along the topographic slope. When flowing over the rough topography, this bottom current generates a 200 m large bottom mixed layer. We further demonstrate that many submesoscale structures are generated at the southernmost tip of the Icelandic shelf, which subsequently spread water masses in the Iceland Basin. These findings have major implication for the understanding of the water masses transport in the North Atlantic, and also for the distribution of benthic species along the Icelandic shelf.

Plain Language Summary Water masses formed in the Arctic Ocean overflow into the North Atlantic at the bottom of the ocean, forming the so-called upper cell of the Atlantic Meridional Overturning Circulation (AMOC). The pathway of the currents carrying these water masses is still under debate due to a lack of observations. In this study, we discuss in details the pathway of these bottom currents in the specific area south of Iceland. We show that a steady current flows along the Icelandic continental shelf, and then divide in smaller structures when reaching the southernmost tip of Iceland. We also show that on its way, the current mixes the bottom layer of the ocean. These findings have major implication in the understanding of heat and carbon transport at depth in this area, which constitute an important response of the climate to anthropogenic forcing.

1. Introduction

The northeastern part of the North Atlantic subpolar gyre is a key part of the Atlantic Meridional Overturning Circulation (AMOC, Buckley & Marshall, 2016). Its so-called "upper cell" ventilates the upper 2 km of the Atlantic Ocean, and it transports heat and carbon from the surface to depths (Kostov et al., 2014; Marshall et al., 2014). It therefore plays a determinant role in the response of the climate to anthropogenic forcing (Drijfhout et al., 2012; Meehl et al., 2014; Winton et al., 2013). The main sources of dense water into the upper cell are overflows from the Nordic Seas (Chafik & Rossby, 2019; Lozier et al., 2019; Tsubouchi et al., 2021). There, intense heat loss in winter transforms the water into colder and denser water masses that subsequently flow southward through gaps in topography (Brakstad, Gebbie, et al., 2023).

While it is the crossroad of this global circulation, the region south of Iceland has been poorly studied in details (see Figure 1a for the location of the places mentioned below). At this place, there is no consensus on the shape and intensity of bottom currents. Studies agree for an overall southwestard flow from the Iceland-Faroe Ridge (IFR) and the Faroe-Bank Channel (FBC) regions toward the Iceland Basin, following the Reykjanes Ridge, see for example, Stow and Holbrook (1984); Bianchi and McCave (1999). When looking at it more precisely, opinions diverge a lot, due to the lack of available data in the area. Investigators sometimes only consider the IFR, the FBC, include an overflow over the Western Valley, or assume a pathway across the deep waters of the Iceland Basin, see for example, Bowles and Jahn (1983); Hansen (1985); Perkins et al. (1998); Hansen and Østerhus (2000, 2007); Beaird et al. (2013); Logemann et al. (2013); Guo et al. (2014); Ullgren et al. (2014); Daniault et al. (2016); Zou et al. (2017); Zhao et al. (2018); Hansen et al. (2018); Petit et al. (2019); Chafik and Rossby (2019); Koman et al. (2022); Brakstad, Gebbie, et al. (2023). Understanding the actual properties of local

Writing – review & editing: Charly de Marez, Angel Ruiz-Angulo, Mathieu Le Corre

geophysical processes at depth is therefore timely. It will allow to better target future in situ observations aiming at quantifying water mass transport and mixing by the bottom currents, and thus better assess deep storage of anthropogenic-induced tracers.

Beyond this slowly-varying and averaged picture, it has been shown in the past years that small-scale processes have an important role in modulating the global ocean properties. This includes submesoscale balanced currents such as Submesoscale Coherent Vortices (SCVs), Intrathermocline Eddies, or fronts (McWilliams, 2019). These structures have been shown to be key for the global heat budget (Su et al., 2018) and the distribution of marine ecosystems (Lévy et al., 2018) via deep-reaching vertical and horizontal transports (Siegelman et al., 2020; Zhong & Bracco, 2013). Small-scale processes also include fine-scale vertical mixing, induced by deep-reaching currents and internal tides flowing over the topography (Gula et al., 2022; Polzin & McDougall, 2022; Vic et al., 2019). These processes are of major importance to regulate the transport of heat and biogeochemical tracers, and they are suggested to be a good candidate for the closing of the oceanic energy budget (de Lavergne et al., 2022; Ferrari & Wunsch, 2009; Jayne, 2009). The contribution of these submesoscale processes in the south Icelandic dynamics has yet not been studied. However, it is likely that they play an important role in the transport of water masses there. Note that the submesoscale is defined here as the scale at which processes happen on horizontal scales smaller than the average deformation radius (here $\mathcal{O}(20-30)$ km (LaCasce & Groeskamp, 2020)), and on vertical scales smaller than the bottom mixed layer (here $\mathcal{O}(100)$ m, see Section 3.2).

In the present paper, we discuss in details the bottom circulation south of Iceland using regional high resolution numerical modeling. In particular we discuss the shape and intensity of the bottom boundary current flowing at ∼1,000 m depth along the Icelandic shelf. This current is the connection between Nordic Seas and the northeastern part of the North Atlantic subpolar gyre. In the following, mention to the "bottom boundary current" refers to this current. We further show that this latter generates numerous submesoscale features on its path and where it overshoots sharp bathymetric structures. This processes are shown to be of importance for the distribution of water masses in the area. In Section 2 we present the methods used to investigate these processes. In Section 3 we present the analysis of the numerical simulations. In Section 4 we discuss and conclude on our results.

2. Methods

2.1. Numerical Simulation of the North Atlantic

We use outputs of a realistic simulation of the North Atlantic Subpolar Gyre, already used and validated in previous studies, for example, Le Corre, Gula, Smilenova, and Houper (2019); Le Corre, Gula, and Treguier (2019); de Marez & Le Corre (n.d.); Smilenova et al. (n.d.); de Marez et al. (2021); Wang et al. (2022). It is performed using the Coastal and Regional Ocean COmmunity model (CROCO, Shchepetkin & McWilliams, 2005, a version of ROMS model). This model solves the hydrostatic primitive equations using the full equation of state for seawater (Shchepetkin & McWilliams, 2011). The horizontal advection terms for tracers and momentum are discretized with third-order upwind advection schemes (UP3), see for example, Klein et al. (2008) for a further description. This parameterization considers implicit dissipation and it damps dispersive errors.

A one-way nesting approach is used. A first simulation of the whole North Atlantic is implemented with a $\Delta x \sim 6$ km horizontal resolution and 50 topography-following levels, such that mesoscale eddies are reasonably well resolved. It is initialized and forced at boundaries with the SODA dataset (Carton & Giese, 2008). At the surface, the forcing is obtained from the daily ERA-INTERIM dataset (Dee et al., 2011). The bathymetry is constructed from the SRTM30 PLUS dataset (Becker et al., 2009). Then, this simulation is used as boundary forcing and initialization for a second —child— simulation in the Subpolar region, with $\Delta x \sim 2$ km horizontal resolution and 80 topography-following levels. This higher resolution resolves small scale bathymetric features. In particular, it allows an accurate description of the FBC and the IFR.

We make use of this high resolution simulation in the present study, for the period 2002–2009 (after a 2-year spin up). Reference to time averaged quantities over this period are denoted $\langle\cdot\rangle_t$. The general features of the simulation throughout the subpolar North Atlantic gyre dynamics, both in the model output and in gridded observations-based products have been validated by Le Corre, Gula, and Treguier (2019). In our domain of interest, a slight average temperature and salinity offset is seen in the whole water column (constant throughout depth). However, it does not affect the average stratification (see Figures 2c and 2d) which is here the main parameter for the study

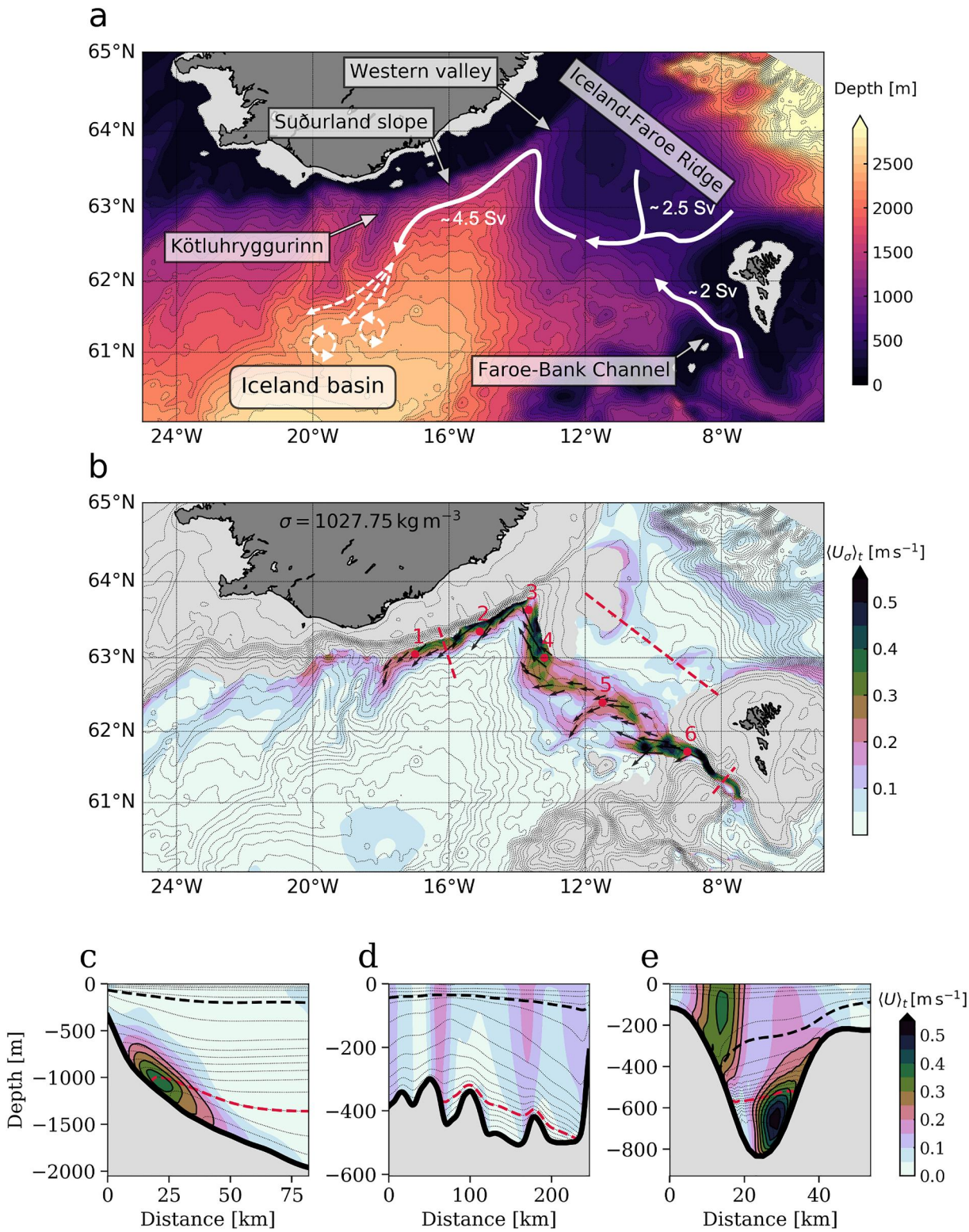

Figure 1. (a) Region of interest, bathymetry, and schematic path of the bottom current; white numbers indicate the transport through the three sections shown in panels (c)–(e). (b) Velocity magnitude on the 1,027.75 kg m^{-3} isopycnal; position of sections shown in panels (c)–(e), position of profiles shown in Figure 2, and bathymetry (thin black lines). (c)–(e): Vertical sections of the velocity magnitude and isopycnals (thin dashed every 0.05 kg m^{-3}, red dashed 1,027.75 kg m^{-3}, and thick dashed σ_{top} = 1,027.3 kg m^{-3}).

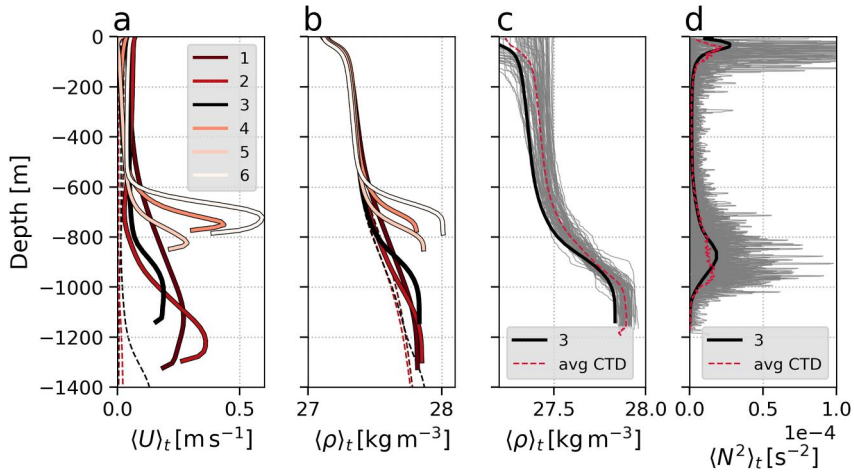

Figure 2. (a) (resp. b): Time-averaged velocity magnitude (resp. potential density) profiles at the locations shown in Figure 1b; thin dashed profiles show profiles ∼50 km off-shore of the same-color profiles. (c) (resp. d): Comparison of potential density (resp. Brunt–Väisälä frequency) profiles between simulation (thick black) and CTD station (thin gray and thick dashed red) at location 3 (Figure 1).

of the dynamical processes. For further details, we refer the reader to Le Corre, Gula, and Treguier (2019)'s description and validation of the simulation, and their Figure 1 that presents the simulation domain.

2.2. Particule Advection Simulations

We perform three offline particle advection simulations, using the velocity field from the numerical simulation on the 1,027.75 kg m^{-3} isopycnal, implementing the set of python classes Parcels (Probably A Really Computationally Efficient Lagrangian Simulator). This tool has been widely used in the past few years and it is fully described in Lange & van Sebille (2017), Delandmeter & van Sebille (2019), and in references therein. The three simulations are designed such that they all are one year long. We arbitrarily chose the year 2005 of the CROCO simulation for the currents.

2.3. In Situ Data

The data used for validation and comparison was obtained from SeaDataNet and the Norwegian Marine Data Center (Brakstad, Våge, et al., 2023) for the region southeast of Iceland, corresponding to 80 CTD profiles from 1996 until 2019 covering the 4 seasons. Most of the profiles were uploaded to these open source databases by the Hydrography Observational Program carried out by the Icelandic Marine and Freshwater Research Institute (Ólafsdóttir et al., 2020). The CTD profiles were used to validate the simulation at the virtual location of 13.7°W and 63.6°N (Stokksnes 5), shown in Figure 1b as the point labeled 3.

3. Results

3.1. General Description of the Bottom Current

Time-averaged simulation outputs show that the bottom boundary current originates from two branches at the northeast boundary of the Iceland Basin. A first branch consists of a northwestward flow coming from the FBC. There, an intense current with average maximum velocity of 0.53 m s^{-1} located below 500 m depth flows along the northern slope of the narrow channel, see Figures 1b and 1e. The transport in this channel has been shown in previous studies to be about 2 Sv (Hansen et al., 2016; Hansen & Østerhus, 2007). We determine that this transport is satisfied when integrating the crossing current between the σ_{top} = 1,027.3 kg m^{-3} isopycnal and the bottom. A second branch consists of a southwestward flow coming from the IFR. There, two weak currents at ∼11°W (on the eastern flank of the westernmost bank) and ∼9°W (on the western flank of the easternmost bank) flow over the ridge. The average maximum velocity of 0.19 m s^{-1} at the bottom is seen at the western most location, see Figures 1b and 1d. The crossing overflow transport between σ_{top} and the bottom is about 2.5 Sv, larger than the FBC transport because of the wider section.

When entering the Iceland Basin, the bottom boundary current stabilizes around the 1,027.75 kg m^{-3} isopycnal, see Figure 1b. It flows northward, constrained along the continental shelf. When reaching the Western Valley, it retroflects following the topography. It then flows southwestward along the continental shelf south of Iceland, namely Suðurland slope, after the name of the Icelandic southern lands. The flow is very well marked along the slope, with average maximum velocity of 0.38 m s^{-1} on the 1,027.75 kg m^{-3} isopycnal, see Figure 1c. This finding justifies the choice of this particular isopycnal for the further investigation of the current made in this study. The transport induced by the current between σ_{top} and the bottom is about 4.5 Sv, thus satisfying the mass conservation from overflows to the Suðurland slope.

Finally, the current overshoots at a submarine cape located ∼18°W,62.5°N. It is called Kötluhryggurinn, "the Katla ridge", after the Katla volcano south of Iceland (Shor, 1980). A slight part of the current overflows west over Kötluhryggurinn, creating weak branches of current further west, see Figure 1b. Further examination of the current using particle advection simulations show that these branches have small impact on the water masses trajectory (Section 3.3). Neither seasonal nor inter-annual variability of the bottom boundary current position/intensity/depth are noticed (not shown), thus justifying the use of 7-year overall time averages.

3.2. Vertical Variations and Mixing at the Bottom

Along its path from the FBC to the Suðurland slope, the current velocity magnitude increases with depth to reach a maximum between ∼0.2 and ∼0.6 m s^{-1}, and then decreases toward the bottom floor over an average thickness between ∼100 m and ∼500 m, see Figure 2a. It dives from ∼700 m depth at the FBC mouth (profile 6) to ∼1,200 m depth at Kötluhryggurinn (profile 1).

A marked Bottom Mixed Layer (BML) is observed along the current path, see Figures 2b–2d, and is confirmed by 24 years of in situ data. This BML is less than 50 m thick at the FBC mouth. It then becomes thicker along the IFR reaching over 200 m in the Western Valley and along the Suðurland slope. The profile three position coincides with the position of CTD casts performed during a 24 years period in the Western Valley (Stokksness 5, Ólafsdóttir et al., 2020). Average vertical profile of potential density from the simulation matches with in situ observations. The slight offset in density is homogeneous on the vertical and is mainly due to a ∼0.5°C temperature offset. Nevertheless, this does not change the dynamics as the stratification (N^2) closely matches thus proving the occurrence of this large BML in the current path, and additionally validating one of the main feature of the simulated current.

The evolution of this BML suggest the combination of frictional and arrested bottom Ekman layers (Brink & Lentz, 2010). The FBC is a narrow-steep-smooth channel which allows the BML to be tightly confined (∼10 km) against the slope; there, the velocity is maximum and the density contrast between the BML and the interior is also the greatest. This bottom boundary current remains confined to the slope throughout the path presented here. First evidence is that this BML is not seen ∼50 km off-shore, outside of the current path, see Figure 2b. Along the path the BML thickness increases coincidentally with the increase in roughness on bottom topography just after the Suðurland slope, which is most likely due to submesoscale viscous processes happening at the bottom, when the current flows over the topography (Polzin et al., 2021).

3.3. The Faith and Spreading of Carried Waters

Two first particle advection simulations confirm that the bottom current originates from both the IFR and the FBC overflows. A total of 6 (resp. 26) particles are released everyday during 300 days along a straight line located in the FBC (resp. on the IFR) on the 1,027.75 kg m^{-3} isopycnal, see Figure 3a. Remarkably, all particles overflowing in the Iceland Basin eventually get trapped along a very narrow path along the Suðurland slope. We then measure the number of particles from each simulation that cross a section perpendicular to the Suðurland slope, see Figure 3a. Some particles do not reach this region at the end of the simulations (34% and 55%); those particles were either advected too slowly or flowing east of the IFR (see dark blue and dark red trajectories in Figure 3a). Nevertheless, when particles released at both locations get trapped in the bottom current they always travel north toward the Western Valley before retroflecting to the west and crossing the Suðurland slope section. Note that an additional backward advection simulation described in Supplementary Information confirms these findings.

Then, a third simulation is designed in which 15 particles are released everyday during a year along a straight line perpendicular to the Suðurland slope on the 1,027.75 kg m^{-3} isopycnal, that is, the same section as the one

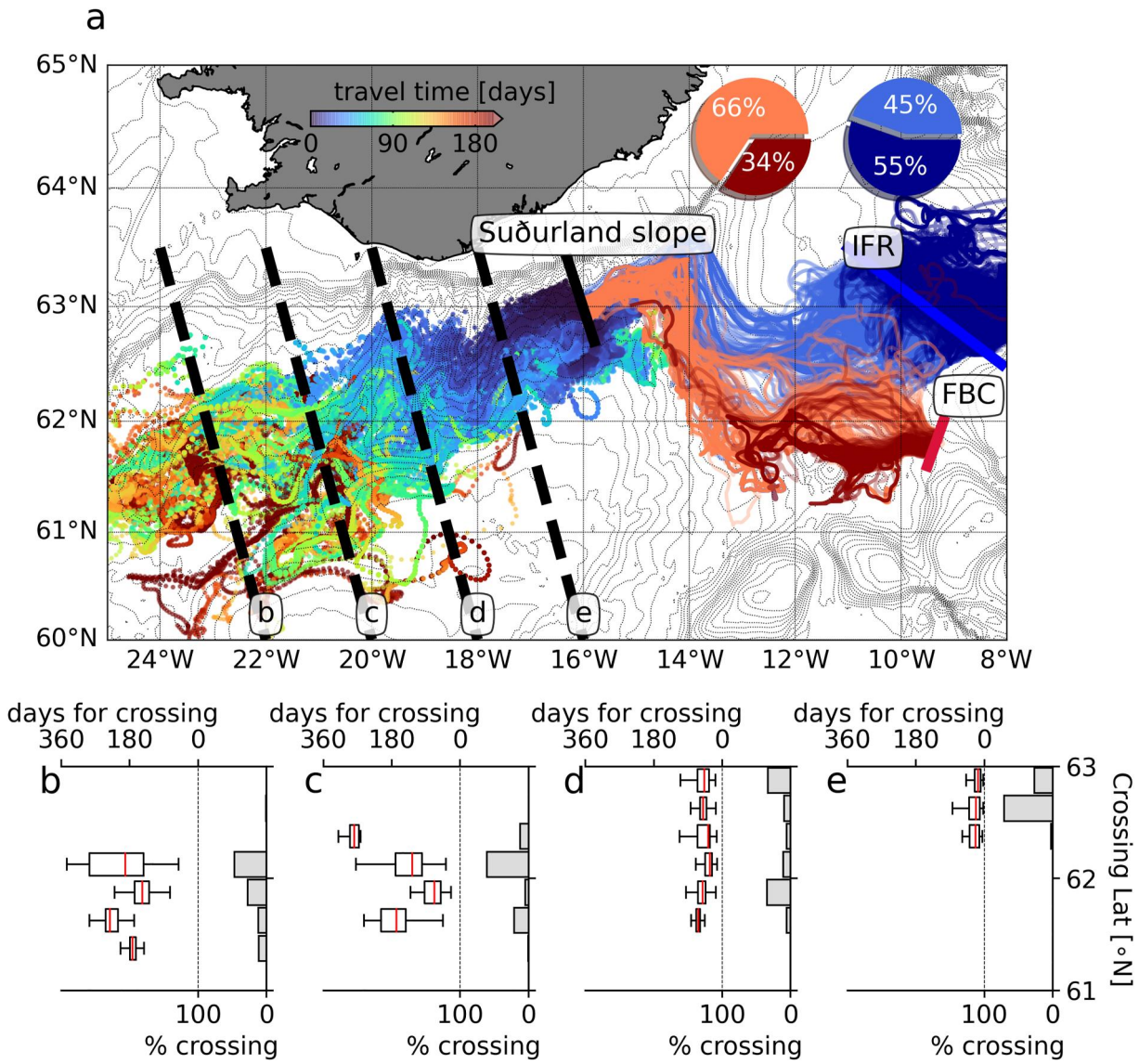

Figure 3. (a) Trajectories of particles (on the 1,027.75 kg m^{-3} isopycnal) released from the IFR (blue), the FBC (red), and the Suðurland slope (rainbow color that indicates the travel time) sections; darker blue (resp. red) show trajectories of particles released from the IFR (resp. FBC) location that dit not cross the Suðurland slope section; for clarity only 1 out of 4 trajectory is shown; pie charts indicate the percentage of trajectories that crossed the Suðurland slope section when released from either the IFR or the FBC locations; black dashed lines indicate the sections used to compute the histograms shown in bottom panels. (b)–(e): Percentage of particles crossing the sections shown in panel (a), and time for the crossing, as a function of latitude.

mentioned previously, see Figure 3a. Particle trajectories from this simulation shows that when reaching Kötluhryggurinn, the waters carried by the bottom current spread out in the Iceland Basin. We measure the latitude and the travel time at which particles cross four different sections, parallel to the launching section, each spaced of 2° in the longitudinal direction, see Figure 3. Particles cross the first section (e) in a few weeks and are concentrated north of 62.5°N, see Figure 3e. After passing Kötluhryggurinn, and as they travel southwestward, they detach from the continental slope, and they cross sections with a large spreading, see Figures 3b–3d. Particles crossing section b are all located south of 62.25°N, and some particles even crossed the 60th parallel North. The spreading is due to turbulent processes, with short time scales, as revealed by the large standard deviations of crossing times. This is also highlighted by the fact that particles are advected by a flow with high values of relative vorticity. In particular, most of the particles have a cyclonic vorticity reaching $\zeta/f > 0.5$ due to the generation of submesoscale structures at Kötluhryggurinn (see Figure S2 in Supporting Information S1). These processes are described in the following section.

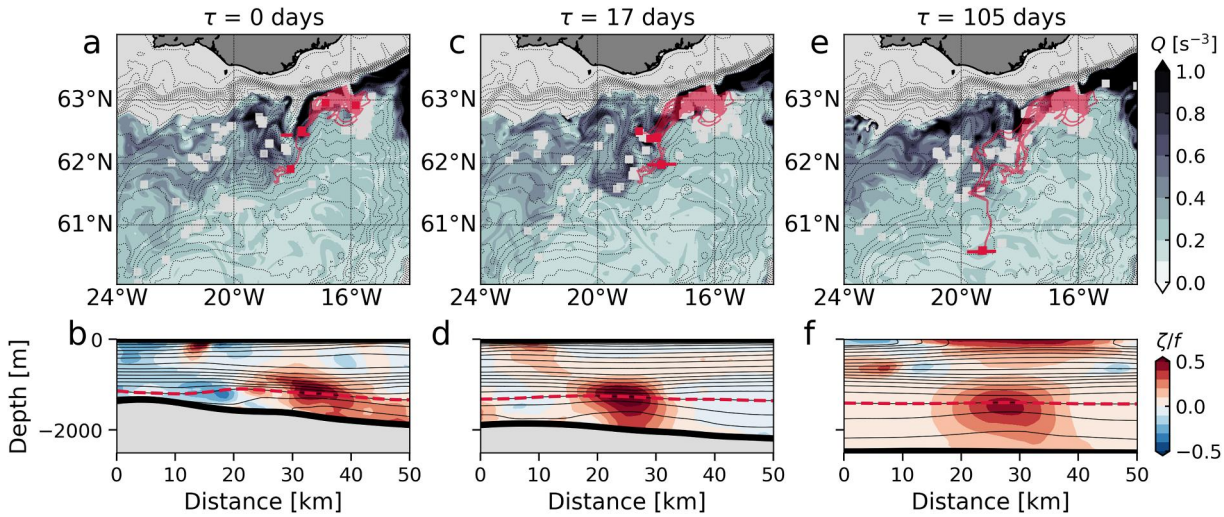

Figure 4. (a), (c) and (e): Snapshots of Ertel Potential Vorticity (divided by 10^9) on the 1,027.75 kg m^{-3} isopycnal; position of particles trapped (resp. don't trapped) by the SCV at $\tau = 105$ days is shown by the red (resp. white) dots. (b), (d), and (f): vertical section of normalized relative vorticity at the position shown by the red dashed lines in top panels; isopycnals are shown in thin black lines; the 1,027.75 kg m^{-3} isopycnal is shown by the thick dashed red line.

3.4. Submesoscale Generation at Kötluhryggurinn

Water masses are spread out in the Iceland Basin by submesoscale structures propagating from Kötluhryggurinn. The mechanism is as follows. The bottom current flows along the Suðurland slope, concentrated around the 1,027.75 kg m^{-3} isopycnal. Viscous interactions (parameterized in the model, see Le Corre, Gula, and Treguier (2019)) with the topography leads to a frictional injection of Potential Vorticity (PV) on this isopycnal. This in turn generates a change of sign of the cross-current PV gradient both horizontally and vertically (see Figure S3 in Supporting Information S1). These are the necessary conditions for Barotropic and Baroclinic instabilities to occur. This results in a highly turbulent flow along the Suðurland slope, as reflected by the high values of Eddy Kinetic Energy (EKE) and Eddy Available Potential Energy (EAPE) on this isopycnal (see Figures S3 and S4 in Supporting Information S1). The flow overshooting at Kötluhryggurinn thus does not follow the slope but meanders south in the Iceland Basin. Water masses are stirred and spread out offshore by intense fronts and rapidly varying flows with —mainly cyclonic— values of vorticity reaching $\zeta/f > 0.5$ (see Figure S2 in Supporting Information S1). Occasionally, the tongue of potential vorticity roll up in the lee of the cape, generating cyclonic SCVs on the 1,027.75 kg m^{-3} isopycnal. This mechanism has already been intensively studied, and identified as an efficient mechanism to form deep submesoscale vortices in Gradient Wind Balance in many places of the ocean (see *e.g.,* D'Asaro, 1988; Dong et al., 2007; Vic et al., 2015; Gula et al., 2015; Morvan et al., 2019; Srinivasan et al., 2019; McWilliams, 2019; Gula et al., 2019; de Marez et al., 2020). We refer the reader to these studies for further details.

The cyclonic SCVs generated at Kötluhryggurinn enhance the spreading of water masses. A particular event of SCV generation is shown in Figure 4. This structure was generated following the mechanism discussed in the previous paragraph. It then traveled south, hundreds of kilometers, carrying water masses offshore. At $\tau = 105$ days (Figures 4e and 4f), 175 particles (out of 5,464 released in total during the simulation) are trapped in its core and travel southward. This represents more than 3% of the total amount of particles present along the Suðurland slope during a year, that have been spread out by this single event. Counting the number of such events is arduous because most of the time generated SCVs merge between each other making the tracking of single structures hazardous. Nevertheless, we report 15–20 events in the year 2005 of the simulation, suggesting that such spreading by submesoscale events is common in this area.

4. Discussion

In this study, we investigated the bottom boundary current flowing in the north of the Iceland Basin. We showed that it originates from both the Faroe-Bank Channel and the Iceland-Faroe Ridge. It then follows the topography on the 1,027.75 kg m^{-3} isopycnal where it induces bottom mixing creating a large Bottom Mixed Layer. It finally

overshoots at Kötluhryggurinn, where submesoscale structures are generated and spread water masses in the open Iceland Basin.

In the past decades, circulation in the northern Iceland Basin has been investigated due to its role in the Atlantic Meridional Overturning Circulation, and numerous schematized views of the bottom circulation have emerged. The present paper aims at suggesting that the bottom circulation of the northern Iceland Basin is as schematized as in Figure 1a, with a current coming from both the Faroe-Bank Channel and the Iceland-Faroe Ridge (with about equal contributions) and flowing along the topographic slope. The exact transport induced by each branch of the current is yet to be determined, and the present study does not allow to provide precise estimates. Future deployment of in situ measurements will go in the way of such transport estimates.

Our study also put forth the fact that when overshooting at Kötluhryggurinn, the bottom current somehow disappears and let place to a submesoscale processes-driven spreading of the water masses in the Iceland Basin, thus unvalidating the view of a current steadily flowing along the Reykjanes Ridge. In particular, a significant amount of water is spread out by locally generated cyclonic SCVs. Even if only a few in situ experiments succeeded in measuring SCVs with a sufficient horizontal resolution (see *e.g.,* L'Hégaret et al., 2016; Meunier et al., 2018; Gula et al., 2019, and references therein), only a few observations of *cyclonic* SCVs were reported (*e.g.,* Bosse et al., 2016; de Marez et al., 2020), suggesting that anticyclonic SCVs are predominant in the deep ocean. Our findings thus further suggest that Kötluhryggurinn is an efficient generation spot for deep intense *cyclonic* SCVs. This result is to be confirmed by in situ measurements in the area to allow further analysis of these submesoscale structures.

The region described in this manuscript is of great importance for the future of the AMOC. Indeed, the dense water carried by the bottom current has enormous importance as it significantly contributes to the lower limb of the AMOC. Moreover, the winter convection there can create surface mixed layer depths over 700 m (Brakstad, Gebbie, et al., 2023), which in some regions allows the exchange of surface waters with dense bottom waters. The upper ocean in this region is warming up and IPCC projections suggest this will continue at even higher rates than other basins (Shu et al., 2022). South of Iceland, the combination of deep mixed layers with warmer surface waters, and thick bottom boundary currents with cold-dense waters may exchange this excess of heat resulting in changes of these dense waters in a warming climate.

The bottom boundary current described in this study also appears to be a key phenomenon to sustain biological activity in the area. Indeed, the distribution of several Cold Water Coral species, in particular *Lophelia pertusa*, strongly coincides with the position of the bottom current we described (see Figure 4 of Buhl-Mortensen et al., 2015). It has been shown in the past that the presence of benthic species, such as Cold Water Coral, is strongly corelated to the physical and chemical properties of seawater. In particular, they rely on a renew of suspended food sources and oxygenated waters, that is, feeding currents (Mienis et al., 2019). The bottom current described here has the potential to act as a enhancement-nutrient-supply current. Its strong intensity efficiently renews the bottom water. The interaction of the current with the topography south of Iceland induces strong vertical gradients, locally enhancing vertical mixing of cold nutrient-rich bottom water to the upper layers. The bottom mixing induced by the current also enhances this water flushing, and contributes in increasing the bottom temperature, necessary condition for this species to survive. This current may have implication to a broader spectrum of benthic species, but more investigation in this direction, and a better sampling of physical-biology-related quantities at the bottom is needed to pursue this question.

Finally, even if it is mainly speculations, it is interesting to draw the question of Kötluhryggurinn formation. Studies have discussed the fact that "The Katla Ridges are smooth features with accumulation of sediment beneath the crests in excess of 1.5 km. Their mode of formation is inferred to result from the rapid denudation of Iceland during the Neogene, sediment transport to the base of the slope by turbidity currents and subsequent entrainment and transport southwestward by the flow of Iceland-Scotland Overflow Water." (Shor, 1980). Even if some other exchanges from the shelf into the canyons may contribute to the sediments, several sources (see *e.g.,* Bowles & Jahn, 1983), suggest that the bottom current has lead to the formation of this bathymetric feature. Taking a step back, this suggests that the bottom current formed Kötluhryggurinn topographic anomaly, which in turn contributed to the generation of submesoscale at this particular place. This could be the signature of geological-timescale forced submesoscale process.

Data Availability Statement

CTD data were provided through SeaDataNet Pan-European infrastructure for ocean and marine data management (https://www.seadatanet.org), and can be downloaded as part of the SDC_ARC_DATA_TS_V2 dataset. Due to the large size of simulation outputs, they are available upon request. A script to reproduce particle advection simulations can be obtained online (de Marez, 2023).

Acknowledgments
C.d.M. was supported by a Queen Margrethe II's and Vigdís Finnbogadóttir's Interdisciplinary Research Centre on Ocean, Climate and Society (ROCS) postdoctoral fellowship. A.R.A. was supported by ROCS. M.L.C. was supported by the French Naval Hydrographic and Oceanographic Service (SHOM) during the writing and by UBO and Région Bretagne through ISblue, Interdisciplinary graduate school for the blue planet (ANR-17-EURE-0015) and co-funded by a grant from the French government under the program "Investissements d'Avenir" during the setup and run of the experiment. Simulations were performed using the HPC facilities DATARMOR of 'Pôle de Calcul Intensif pour la Mer' at Ifremer, Brest, France. We would like to acknowledge the significant effort invested in acquiring and maintaining the Hydrography Observational Programme by the Icelandic Marine and Freshwater Research Institute.

References

Beaird, N., Rhines, P., & Eriksen, C. (2013). Overflow waters at the Iceland–Faroe Ridge observed in multiyear seaglider surveys. *Journal of Physical Oceanography*, *43*(11), 2334–2351. https://doi.org/10.1175/jpo-d-13-029.1

Becker, J. J., Sandwell, D. T., Smith, W. H. F., Braud, J., Binder, B., Depner, J., et al. (2009). Global bathymetry and elevation data at 30 arc seconds resolution: SRTM30_plus. *Marine Geodesy*, *32*(4), 355–371. https://doi.org/10.1080/01490410903297766

Bianchi, G. G., & McCave, I. N. (1999). Holocene periodicity in North Atlantic climate and deep-ocean flow south of Iceland. *Nature*, *397*(6719), 515–517. https://doi.org/10.1038/17362

Bosse, A., Testor, P., Houpert, L., Damien, P., Prieur, L., Hayes, D., et al. (2016). Scales and dynamics of submesoscale Coherent Vortices formed by deep convection in the northwestern Mediterranean Sea: Vortices in the NW Mediterranean Sea. *Journal of Geophysical Research: Oceans*, *121*(10), 7716–7742. https://doi.org/10.1002/2016JC012144

Bowles, F. A., & Jahn, W. H. (1983). Geological/geophysical observations and inferred bottom-current flow: South flank Iceland—Faeroe Ridge. *Marine Geology*, *52*(3–4), 159–185. https://doi.org/10.1016/0025-3227(83)90054-3

Brakstad, A., Gebbie, G., Våge, K., Jeansson, E., & Ólafsdóttir, S. R. (2023). Formation and pathways of dense water in the Nordic Seas based on a regional inversion. *Progress in Oceanography*, *212*, 102981. https://doi.org/10.1016/j.pocean.2023.102981

Brakstad, A., Våge, K., Ólafsdóttir, S. R., Jeansson, E., & Gebbie, G. (2023). Hydrographic and geochemical observations in the nordic seas between 1950 and 2019. https://doi.org/10.21335/NMDC-1271328906.102981

Brink, K. H., & Lentz, S. J. (2010). Buoyancy arrest and bottom ekman transport. Part I: Steady flow. *Journal of Physical Oceanography*, *40*(4), 621–635. https://doi.org/10.1175/2009jpo4266.1

Buckley, M. W., & Marshall, J. (2016). Observations, inferences, and mechanisms of the Atlantic Meridional Overturning Circulation: A review. *Reviews of Geophysics*, *54*(1), 5–63. https://doi.org/10.1002/2015rg000493

Buhl-Mortensen, L., Olafsdottir, S. H., Buhl-Mortensen, P., Burgos, J. M., & Ragnarsson, S. A. (2015). Distribution of nine cold-water coral species (Scleractinia and Gorgonacea) in the cold temperate North Atlantic: Effects of bathymetry and hydrography. *Hydrobiologia*, *759*(1), 39–61. https://doi.org/10.1007/s10750-014-2116-x

Carton, J. A., & Giese, B. S. (2008). A reanalysis of ocean climate using Simple Ocean Data Assimilation (SODA). *Monthly Weather Review*, *136*(8), 2999–3017. https://doi.org/10.1175/2007MWR1978.1

Chafik, L., & Rossby, T. (2019). Volume, heat, and freshwater divergences in the subpolar North Atlantic suggest the Nordic Seas as key to the state of the meridional overturning circulation. *Geophysical Research Letters*, *46*(9), 4799–4808. https://doi.org/10.1029/2019gl082110

Daniault, N., Mercier, H., Lherminier, P., Sarafanov, A., Falina, A., Zunino, P., et al. (2016). The northern North Atlantic Ocean mean circulation in the early 21st century. *Progress in Oceanography*, *146*, 142–158. https://doi.org/10.1016/j.pocean.2016.06.007

D'Asaro, E. A. (1988). Generation of submesoscale vortices: A new mechanism. *Journal of Geophysical Research*, *93*(C6), 6685–6693. https://doi.org/10.1029/jc093ic06p06685

Dee, D. P., Uppala, S. M., Simmons, A. J., Berrisford, P., Poli, P., Kobayashi, S., et al. (2011). The ERA-interim reanalysis: Configuration and performance of the data assimilation system. *Quarterly Journal of the Royal Meteorological Society*, *137*(656), 553–597. https://doi.org/10.1002/qj.828

Delandmeter, P., & van Sebille, E. (2019). The Parcels v2.0 Lagrangian framework: New field interpolation schemes. *Geoscientific Model Development*, *12*(8), 3571–3584. https://doi.org/10.5194/gmd-12-3571-2019

de Lavergne, C., Groeskamp, S., Zika, J., & Johnson, H. L. (2022). The role of mixing in the large-scale ocean circulation. In *Ocean Mixing* (pp. 35–63).

de Marez, C. (2023). demarez/data: Release lagpart_run for katla current (V.2.0.0) [Software]. Zenodohttps://doi.org/10.5281/zenodo.10216043

de Marez, C., Carton, X., Corréard, S., l'Hégaret, P., & Morvan, M. (2020). Observations of a deep submesoscale cyclonic vortex in the Arabian sea. *Geophysical Research Letters*, *47*(13), e2020GL087881. https://doi.org/10.1029/2020gl087881

de Marez, C., & Le Corre, M. Can the earth be flat? A physical oceanographer's perspective. (n.d.).

de Marez, C., Le Corre, M., & Gula, J. (2021). The influence of merger and convection on an anticyclonic eddy trapped in a bowl. *Ocean Modelling*, *167*, 101874. https://doi.org/10.1016/j.ocemod.2021.101874

Dong, C., McWilliams, J. C., & Shchepetkin, A. F. (2007). Island wakes in deep water. *Journal of Physical Oceanography*, *37*(4), 962–981. https://doi.org/10.1175/jpo3047.1

Drijfhout, S., Van Oldenborgh, G. J., & Cimatoribus, A. (2012). Is a decline of AMOC causing the warming hole above the North Atlantic in observed and modeled warming patterns? *Journal of Climate*, *25*(24), 8373–8379. https://doi.org/10.1175/jcli-d-12-00490.1

Ferrari, R., & Wunsch, C. (2009). Ocean circulation kinetic energy: Reservoirs, sources, and sinks. *Annual Review of Fluid Mechanics*, *41*(1), 253–282. https://doi.org/10.1146/annurev.fluid.40.111406.102139

Gula, J., Blacic, T. M., & Todd, R. E. (2019). Submesoscale Coherent vortices in the gulf stream. *Geophysical Research Letters*, *46*(5), 2704–2714. https://doi.org/10.1029/2019GL081919

Gula, J., Molemaker, M. J., & McWilliams, J. C. (2015). Topographic vorticity generation, submesoscale instability and vortex street formation in the Gulf Stream. *Geophysical Research Letters*, *42*(10), 4054–4062. https://doi.org/10.1002/2015gl063731

Gula, J., Taylor, J., Shcherbina, A., & Mahadevan, A. (2022). *Submesoscale processes and mixing* In *Ocean Mixing* (pp. 181–214). Elsevier.

Guo, C., Ilicak, M., Fer, I., Darelius, E., & Bentsen, M. (2014). Baroclinic instability of the Faroe Bank Channel overflow. *Journal of Physical Oceanography*, *44*(10), 2698–2717. https://doi.org/10.1175/jpo-d-14-0080.1

Hansen, B. (1985). The circulation of the northern part of the Northeast Atlantic. *Rit. Fisk.*, *9*, 110–126.

Hansen, B., Húsgarð Larsen, K. M., Hátún, H., & Østerhus, S. (2016). A stable Faroe Bank Channel overflow 1995–2015. *Ocean Science*, *12*(6), 1205–1220. https://doi.org/10.5194/os-12-1205-2016

Hansen, B., Larsen, K. M. H., Olsen, S. M., Quadfasel, D., Jochumsen, K., & Østerhus, S. (2018). Overflow of cold water across the Iceland–Faroe Ridge through the Western Valley. *Ocean Science*, *14*(4), 871–885. https://doi.org/10.5194/os-14-871-2018

Hansen, B., & Østerhus, S. (2000). North Atlantic–Nordic seas exchanges. *Progress in Oceanography*, *45*(2), 109–208. https://doi.org/10.1016/s0079-6611(99)00052-x

Hansen, B., & Østerhus, S. (2007). Faroe bank channel overflow 1995–2005. *Progress in Oceanography*, *75*(4), 817–856. https://doi.org/10.1016/j.pocean.2007.09.004

Jayne, S. R. (2009). The impact of abyssal mixing parameterizations in an ocean general circulation model. *Journal of Physical Oceanography*, *39*(7), 1756–1775. https://doi.org/10.1175/2009jpo4085.1

Klein, P., Hua, B. L., Lapeyre, G., Capet, X., Le Gentil, S., & Sasaki, H. (2008). Upper ocean turbulence from high-resolution 3D simulations. *Journal of Physical Oceanography*, *38*(8), 1748–1763. https://doi.org/10.1175/2007jpo3773.1

Koman, G., Johns, W., Houk, A., Houpert, L., & Li, F. (2022). Circulation and overturning in the eastern North Atlantic subpolar gyre. *Progress in Oceanography*, *208*, 102884. https://doi.org/10.1016/j.pocean.2022.102884

Kostov, Y., Armour, K. C., & Marshall, J. (2014). Impact of the Atlantic meridional overturning circulation on ocean heat storage and transient climate change. *Geophysical Research Letters*, *41*(6), 2108–2116. https://doi.org/10.1002/2013gl058998

LaCasce, J. H., & Groeskamp, S. (2020). Baroclinic modes over rough bathymetry and the surface deformation radius. *Journal of Physical Oceanography*, *50*(10), 2835–2847. https://doi.org/10.1175/jpo-d-20-0055.1

Lange, M., & van Sebille, E. (2017). Parcels v0.9: Prototyping a Lagrangian ocean analysis framework for the petascale age. *Geoscientific Model Development*, *10*(11), 4175–4186. https://doi.org/10.5194/gmd-10-4175-2017

Le Corre, M., Gula, J., Smilenova, A., & Houper, L. (2019). On the dynamics of a deep quasi-permanent anticylonic eddy in the rockall trough. In *French Congress of Mechanics*.

Le Corre, M., Gula, J., & Treguier, A. M. (2019). Barotropic vorticity balance of the north Atlantic subpolar gyre in an eddy-resolving model. *Ocean Science*. https://doi.org/10.5194/os-2019-114

Lévy, M., Franks, P. J., & Smith, K. S. (2018). The role of submesoscale currents in structuring marine ecosystems. *Nature Communications*, *9*(1), 4758. https://doi.org/10.1038/s41467-018-07059-3

L'Hégaret, P., Carton, X., Louazel, S., & Boutin, G. (2016). Mesoscale eddies and submesoscale structures of Persian Gulf Water off the Omani coast in spring 2011. *Ocean Science*, *12*(3), 687–701. https://doi.org/10.5194/os-12-687-2016

Logemann, K., Ólafsson, J., Snorrason, Á., Valdimarsson, H., & Marteinsdóttir, G. (2013). The circulation of Icelandic waters–a modelling study. *Ocean Science*, *9*(5), 931–955. https://doi.org/10.5194/os-9-931-2013

Lozier, M. S., Li, F., Bacon, S., Bahr, F., Bower, A. S., Cunningham, S., et al. (2019). A sea change in our view of overturning in the subpolar North Atlantic. *Science*, *363*(6426), 516–521. https://doi.org/10.1126/science.aau6592

Marshall, J., Armour, K. C., Scott, J. R., Kostov, Y., Hausmann, U., Ferreira, D., et al. (2014). The ocean's role in polar climate change: Asymmetric arctic and Antarctic responses to greenhouse gas and ozone forcing. *Philosophical Transactions of the Royal Society A: Mathematical, Physical & Engineering Sciences*, *372*(2019), 20130040. https://doi.org/10.1098/rsta.2013.0040

McWilliams, J. C. (2019). A survey of submesoscale currents. *Geoscience Letters*, *6*(1), 3. https://doi.org/10.1186/s40562-019-0133-3

Meehl, G. A., Goddard, L., Boer, G., Burgman, R., Branstator, G., Cassou, C., et al. (2014). Decadal climate prediction: An update from the trenches. *Bulletin of the American Meteorological Society*, *95*(2), 243–267. https://doi.org/10.1175/bams-d-12-00241.1

Meunier, T., Tenreiro, M., Pallàs-Sanz, E., Ochoa, J., Ruiz-Angulo, A., Portela, E., et al. (2018). Intrathermocline eddies embedded within an anticyclonic vortex ring. *Geophysical Research Letters*, *45*(15), 7624–7633. https://doi.org/10.1029/2018GL077527

Mienis, F., Bouma, T., Witbaard, R., Van Oevelen, D., & Duineveld, G. (2019). Experimental assessment of the effects of coldwater coral patches on water flow. *Marine Ecology Progress Series*, *609*, 101–117. https://doi.org/10.3354/meps12815

Morvan, M., L'Hégaret, P., Carton, X., Gula, J., Vic, C., de Marez, C., et al. (2019). The life cycle of submesoscale eddies generated by topographic interactions. *Ocean Science*, *15*(6), 1531–1543. https://doi.org/10.5194/os-15-1531-2019

Ólafsdóttir, S. R., Danielsen, M., Ólafsdóttir, E., Benoit-Cattin, A., Sliwinski, J., & Macrander, A. (2020). *Ástand sjávar 2017 og 2018*. Haf-og vatnarannsóknir.

Perkins, H., Hopkins, T., Malmberg, S.-A., Poulain, P.-M., & Warn-Varnas, A. (1998). Oceanographic conditions east of Iceland. *Journal of Geophysical Research*, *103*(C10), 21531–21542. https://doi.org/10.1029/98jc00890

Petit, T., Mercier, H., & Thierry, V. (2019). New insight into the formation and evolution of the East Reykjanes Ridge current and Irminger current. *Journal of Geophysical Research: Oceans*, *124*(12), 9171–9189. https://doi.org/10.1029/2019jc015546

Polzin, K. L., & McDougall, T. J. (2022). *Mixing at the ocean's bottom boundary*. In *Ocean Mixing* (pp. 145–180). Elsevier.

Polzin, K. L., Wang, B., Wang, Z., Thwaites, F., & Williams, A. J., III. (2021). Moored flux and dissipation estimates from the northern deepwater gulf of Mexico. *Fluids*, *6*(7), 237. https://doi.org/10.3390/fluids6070237

Shchepetkin, A. F., & McWilliams, J. C. (2005). The regional oceanic modeling system (ROMS): A split-explicit, free-surface, topography-following-coordinate oceanic model. *Ocean Modelling*, *9*(4), 347–404. https://doi.org/10.1016/j.ocemod.2004.08.002

Shchepetkin, A. F., & McWilliams, J. C. (2011). Accurate Boussinesq oceanic modeling with a practical, "Stiffened" Equation of State. *Ocean Modelling*, *38*(1–2), 41–70. https://doi.org/10.1016/j.ocemod.2011.01.010

Shor, A. N. (1980). *Bottom currents and abyssal sedimentation processes south of Iceland*. (Doctoral dissertation). Massachusetts Institute of Technology. Retrieved from https://dspace.mit.edu/handle/1721.1/58122

Shu, Q., Wang, Q., Årthun, M., Wang, S., Song, Z., Zhang, M., & Qiao, F. (2022). Arctic ocean amplification in a warming climate in CMIP6 models. *Science Advances*, *8*(30), eabn9755. https://doi.org/10.1126/sciadv.abn9755

Siegelman, L., Klein, P., Rivière, P., Thompson, A. F., Torres, H. S., Flexas, M., & Menemenlis, D. (2020). Enhanced upward heat transport at deep submesoscale ocean fronts. *Nature Geoscience*, *13*(1), 50–55. https://doi.org/10.1038/s41561-019-0489-1

Smilenova, A., Gula, J., Le Corre, M., Houpert, L., & Reecht, Y. A persistent deep anticyclonic vortex in the rockall trough sustained by anticyclonic vortices shed from the slope current and wintertime convection. (n.d.).

Srinivasan, K., McWilliams, J. C., Molemaker, M. J., & Barkan, R. (2019). Submesoscale vortical wakes in the Lee of topography. *Journal of Physical Oceanography*, *49*(7), 1949–1971. https://doi.org/10.1175/JPO-D-18-0042.1

Stow, D., & Holbrook, J. (1984). North Atlantic contourites: An overview. *Geological Society, London, Special Publications*, *15*(1), 245–256. https://doi.org/10.1144/gsl.sp.1984.015.01.16

Su, Z., Wang, J., Klein, P., Thompson, A. F., & Menemenlis, D. (2018). Ocean submesoscales as a key component of the global heat budget. *Nature Communications*, *9*(1), 775. https://doi.org/10.1038/s41467-018-02983-w

Tsubouchi, T., Våge, K., Hansen, B., Larsen, K. M. H., Østerhus, S., Johnson, C., et al. (2021). Increased ocean heat transport into the Nordic Seas and Arctic Ocean over the period 1993–2016. *Nature Climate Change*, *11*(1), 21–26. https://doi.org/10.1038/s41558-020-00941-3

Ullgren, J. E., Fer, I., Darelius, E., & Beaird, N. (2014). Interaction of the Faroe Bank Channel overflow with Iceland Basin intermediate waters. *Journal of Geophysical Research: Oceans*, *119*(1), 228–240. https://doi.org/10.1002/2013jc009437

Vic, C., Naveira Garabato, A. C., Green, J. M., Waterhouse, A. F., Zhao, Z., Melet, A., et al. (2019). Deep-ocean mixing driven by small-scale internal tides. *Nature Communications*, *10*(1), 2099. https://doi.org/10.1038/s41467-019-10149-5

Vic, C., Roullet, G., Capet, X., Carton, X., Molemaker, M. J., & Gula, J. (2015). Eddy-topography interactions and the fate of the Persian Gulf Outflow: PERSIAN GULF OUTFLOW. *Journal of Geophysical Research: Oceans*, *120*(10), 6700–6717. https://doi.org/10.1002/2015jc011033

Wang, L., Gula, J., Collin, J., & Mémery, L. (2022). Effects of mesoscale dynamics on the path of fast-sinking particles to the deep ocean: A modeling study. *Journal Of Geophysical Research-oceans*, *127*(7). https://doi.org/10.1029/2022jc018799

Winton, M., Griffies, S. M., Samuels, B. L., Sarmiento, J. L., & Frölicher, T. L. (2013). Connecting changing ocean circulation with changing climate. *Journal of Climate*, *26*(7), 2268–2278. https://doi.org/10.1175/jcli-d-12-00296.1

Zhao, J., Bower, A., Yang, J., Lin, X., & Penny Holliday, N. (2018). Meridional heat transport variability induced by mesoscale processes in the subpolar North Atlantic. *Nature Communications*, *9*(1), 1124. https://doi.org/10.1038/s41467-018-03134-x

Zhong, Y., & Bracco, A. (2013). Submesoscale impacts on horizontal and vertical transport in the gulf of Mexico. *Journal of Geophysical Research: Oceans*, *118*(10), 5651–5668. https://doi.org/10.1002/jgrc.20402

Zou, S., Lozier, S., Zenk, W., Bower, A., & Johns, W. (2017). Observed and modeled pathways of the Iceland Scotland Overflow Water in the eastern North Atlantic. *Progress in Oceanography*, *159*, 211–222. https://doi.org/10.1016/j.pocean.2017.10.003